Electronic Supporting Information

Control of Reactivity through Chemical Order in Very Small RuRe Nanoparticles

Tuğçe Ayvalı, [ab] *Pier-Francesco Fazzini,* [c] *Pierre Lecante,* [d] *Alvaro Mayoral,* [e] *Karine Philippot* [ab,]* *and Bruno Chaudret* [c,]*

[a] Laboratoire de Chimie de Coordination ; CNRS ; LCC ; 205 Route de Narbonne ; F-31077 Toulouse (France) and Université de Toulouse;

[b] UPS, INPT, LCC ; F-31077 Toulouse (France)

[c] LPCNO; Laboratoire de Physique et Chimie des Nano-Objets, UMR 5215 INSA-CNRS-UPS, Institut des Sciences Appliquées, 135 Avenue de Rangueil, F-31077 Toulouse (France)

[d] CNRS UPR 8011; CEMES (Centre d'Elaboration des Matériaux et d'Etudes Structurales) 29 Rue Jeanne Marvig, F- 31055 Toulouse (France)

[e] LMA, Laboratorio de Microscopias Avanzadas, Instituto de Nanociencia de Aragon (INA), Universidad de Zaragoza, Campus Río Ebro C/ Mariano Esquillor s/n, 50018 Zaragoza, Spain

Corresponding Authors

*Karine Philippot, E-mail: karine.philippot@lcc-toulouse.fr

*Bruno Chaudret, E-mail: chaudret@insa-toulouse.fr

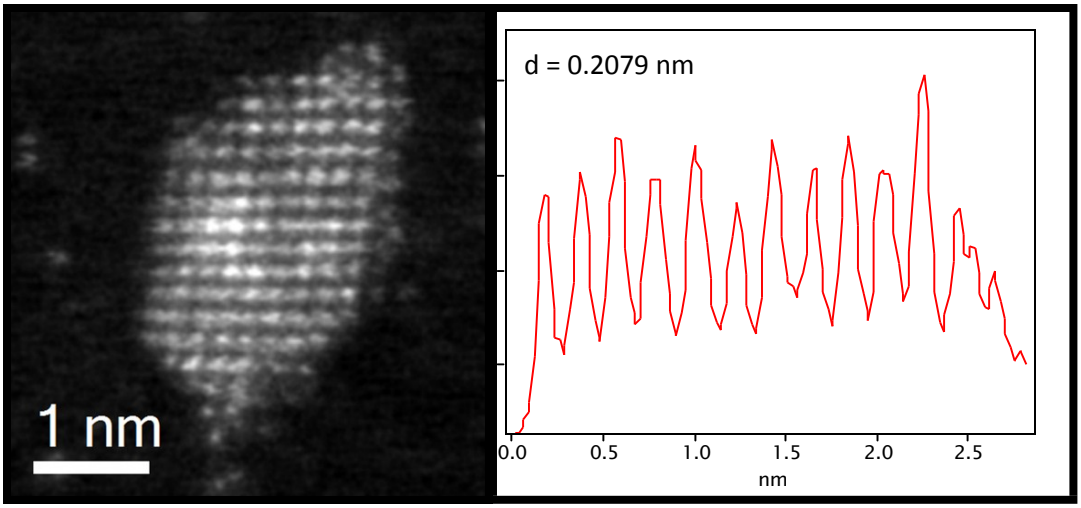

Fig. S1 STEM image of an alloy type RuRe/PVP NPs (left) and corresponding interplanar distance analysis (right).

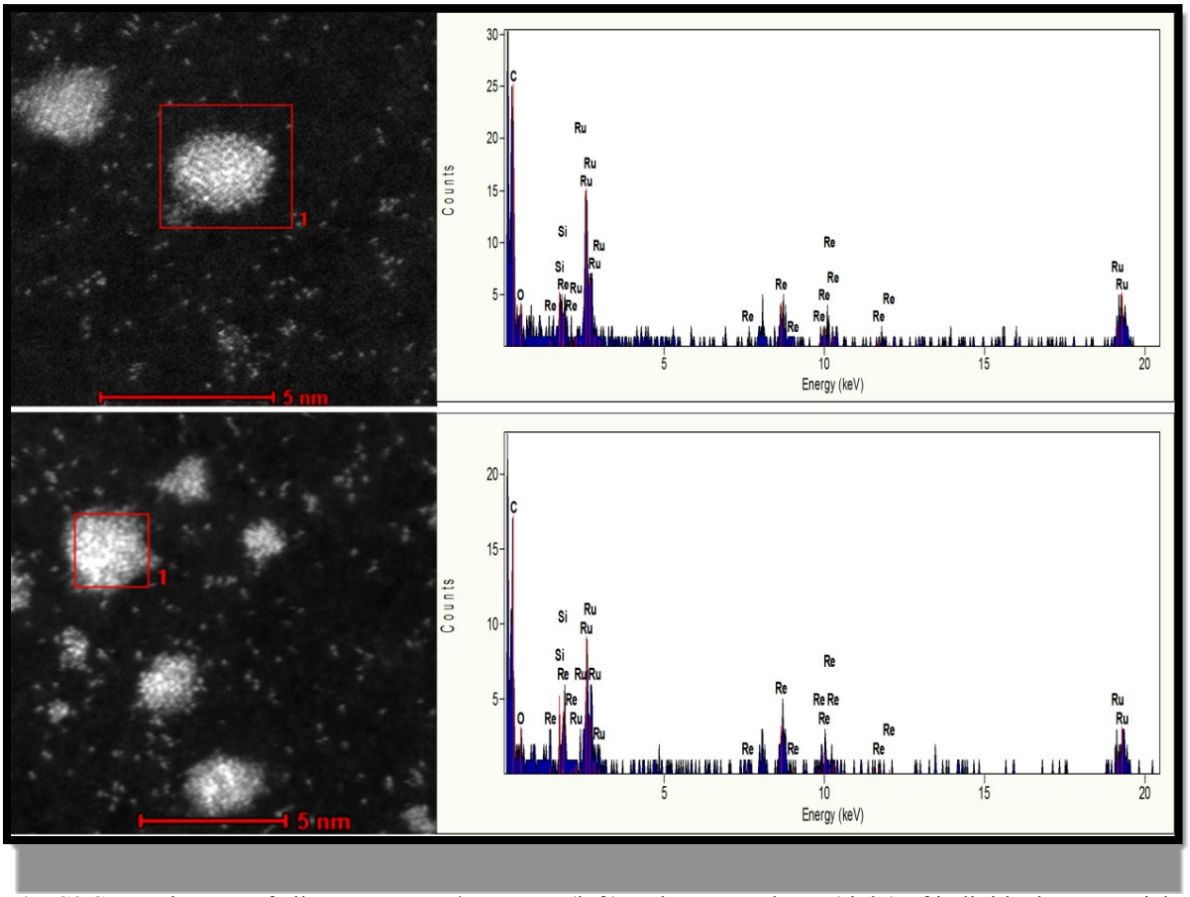

Fig. S2 STEM images of alloy type RuRe/PVP NPs (left) and EDX analyses (right) of individual nanoparticles highlighted with red frame.

^{1}H-NMR study of the decomposition of [Ru(COD)(COT)] and [$Re_2(C_3H_5)_4$]

The reaction was performed in an air-tight high pressure NMR tube, with the same molar concentration of metals and PVP (Ru:Re 1:1 molar ratio, total 10 wt.% metal in PVP) dissolved in deuterated THF (d_8-THF). First an NMR spectrum was recorded from the crude solution without pressurizing the tube with H_2, Then, the NMR tube was pressurized with 3 bar H_2 at r.t. and ^{1}H-NMR spectra were recorded every 15 min automatically **(Fig. S3).** First at r.t., disappearing of olefin ligand signals (δ= 5.7 (m), 5.1 (m), 3.8 (m), 2.9 (m), 2.1 (m), 0.9 (m) ppm) and appearance of cyclooctane peak (δ= 1.53 ppm) were observed without any significant change in the intensity of the peaks of [$Re_2(C_3H_5)_4$] (δ= 5.6 (m), 3.9 (t) and -0.9 (dd) ppm). At r.t., no significant change was observed in the intensity of proton peaks coming from [$Re_2(C_3H_5)_4$]. Therefore, after the consumption of all [Ru(COD)(COT)], the reaction mixture was again pressurized with H_2 and the temperature was increased to 60^{o}C inside the NMR instrument. Then, the disappearance of the peaks of [$Re_2(C_3H_5)_4$] could be observed clearly together with the evolution of dissolved H_2 in the solution (δ= 4.55 ppm). The NMR experiments confirmed that the applied reaction conditions allowed the sequential decomposition of [Ru(COD)(COT)] (first) and [$Re_2(C_3H_5)_4$] (second).

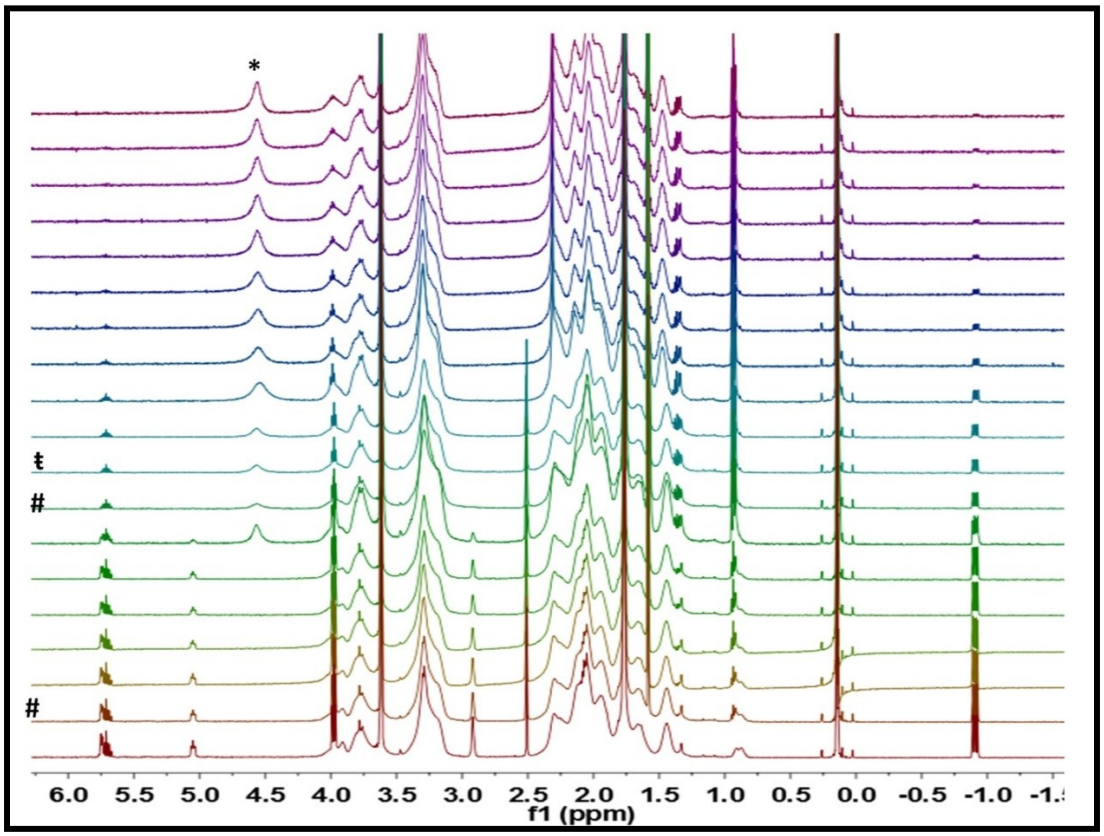

Fig. S3 ^{1}H-NMR study of the decomposition of [Ru(COD)(COT)] and [$Re_2(C_3H_5)_4$] mixture under 3 bar H_2 in the presence of PVP (stabilizer) and d_8-THF (solvent) inside an air-tight high pressure NMR tube. # Pressurizing the tube with 3 bar H_2. * Peak of dissolved H_2. t Increasing the temperature to 60^{o}C.

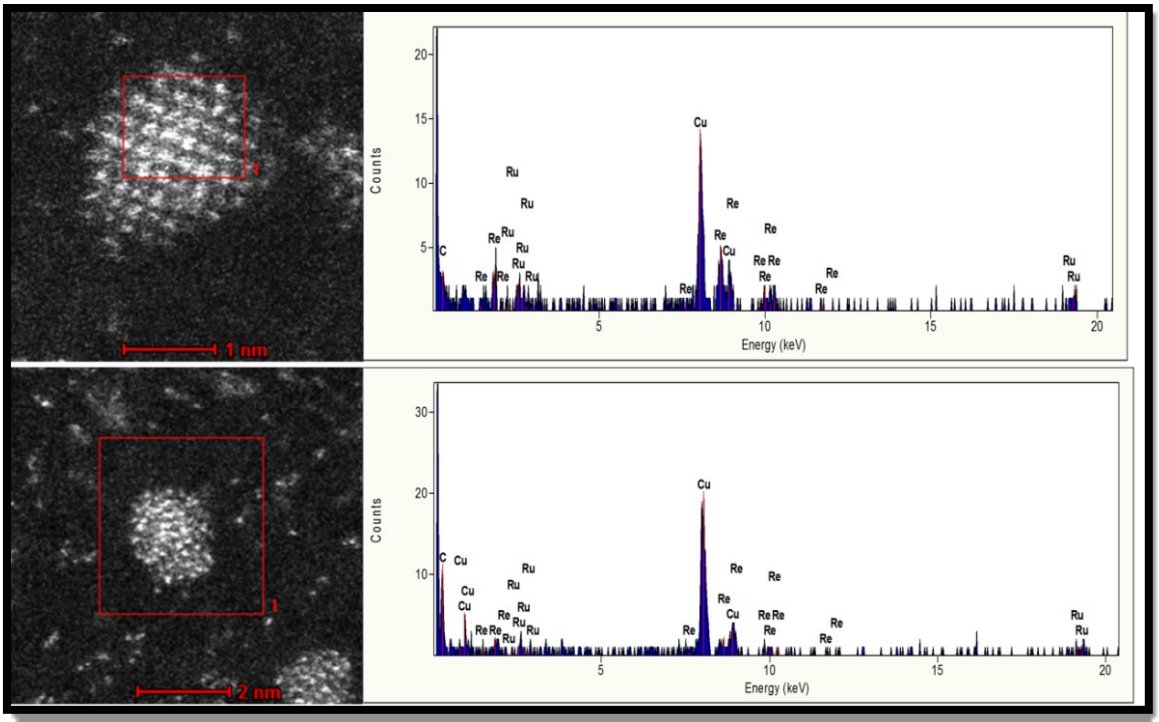

Fig. S4 STEM images of core-shell type RuRe/PVP NPs (left) and EDX analyses (right) of individual nanoparticles highlighted with red frame.

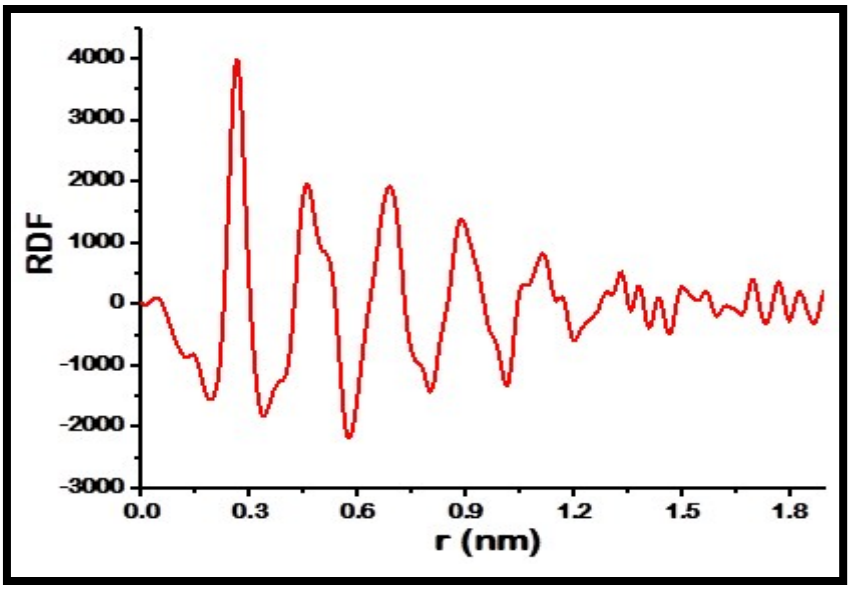

Fig. S5 RDF of core-shell type RuRe/PVP NPs obtained by WAXS.

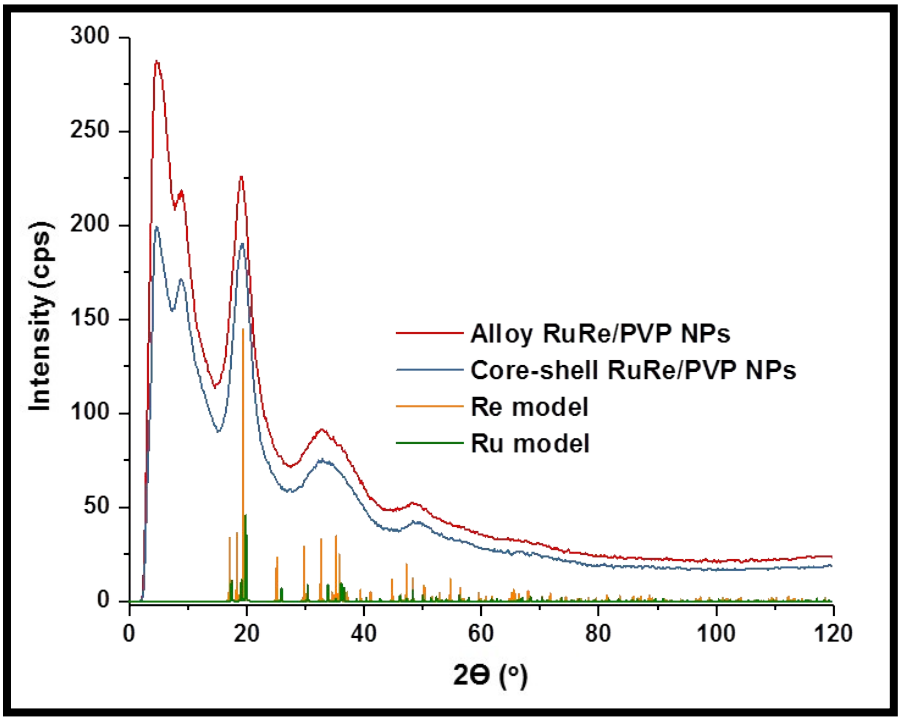

Fig. S6 Comparison of XRD diffractograms of alloy and core-shell RuRe/PVP NPs.

WAXS patterns in the reciprocal space present only very broad peaks as expected for very small particles (Fig. S6). However, the intensity patterns are in good agreement with hcp structure of bulk Re and Ru, based on values taken from ICSD and RDFs computed for hcp model according to Ru and Re (please refer to *Chem. Commun.*, 2014, 50, 10809–11 and *J. Am. Chem. Soc.*, Vol. 123, No. 31, 2001).

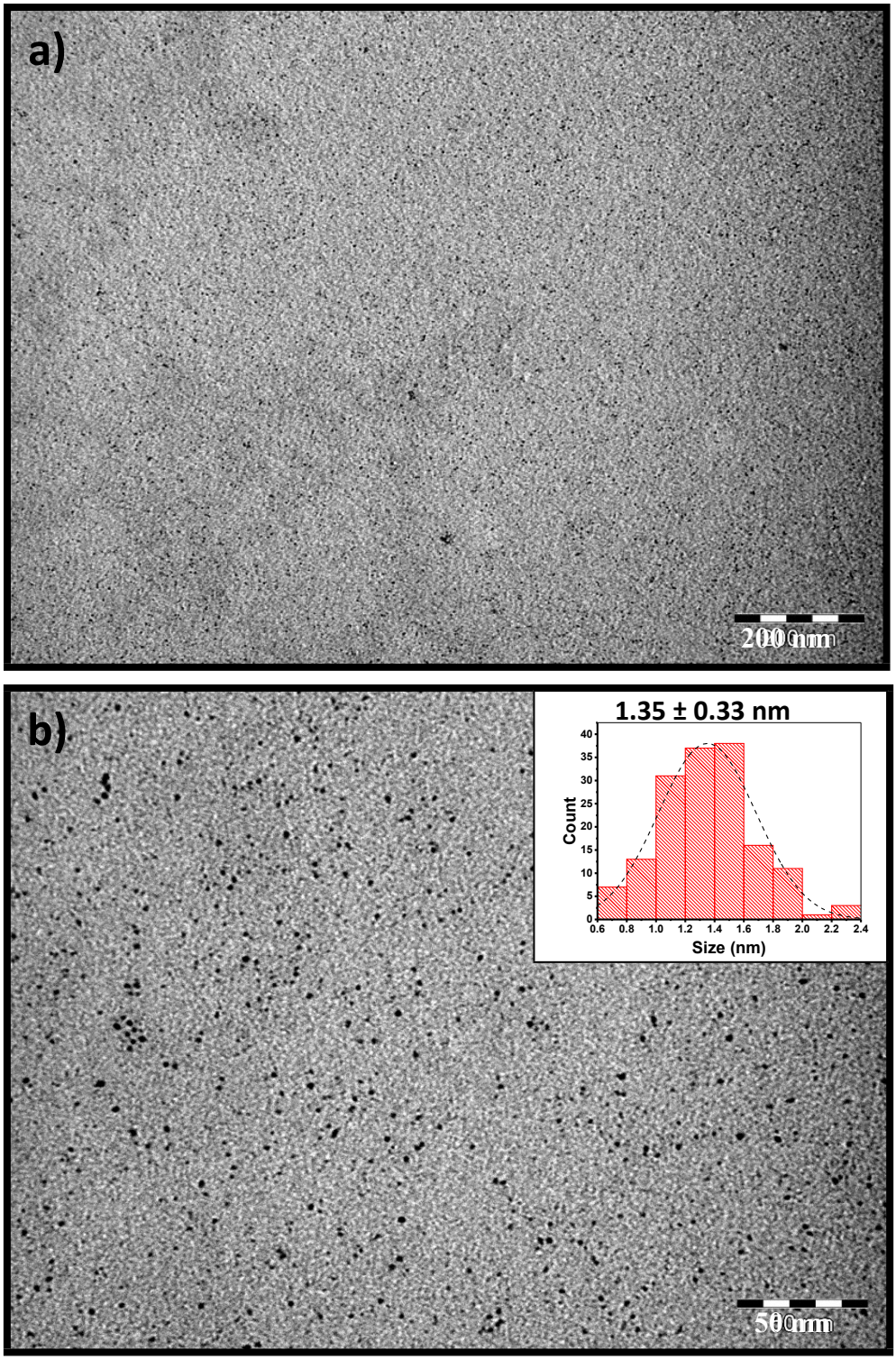

Fig. S7 a-b) TEM images of alloy type RuRe/PVP NPs after CO adsorption at lower and higher magnifications. Inset: Size histogram built from image b.

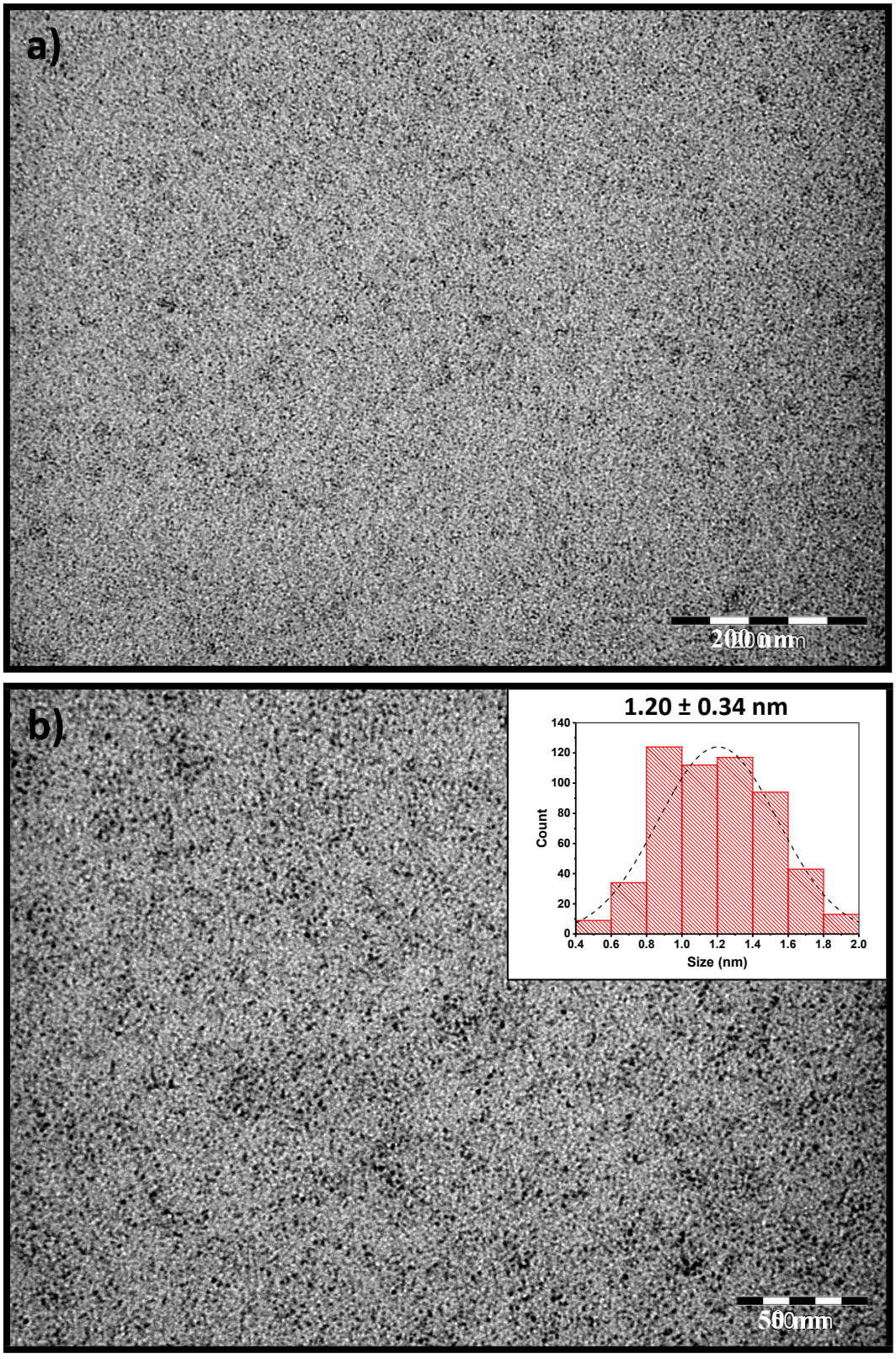

Fig. S8 a-b) TEM images of core-shell type RuRe/PVP NPs after CO adsorption at lower and higher magnifications. Inset: Size histogram built from image b.

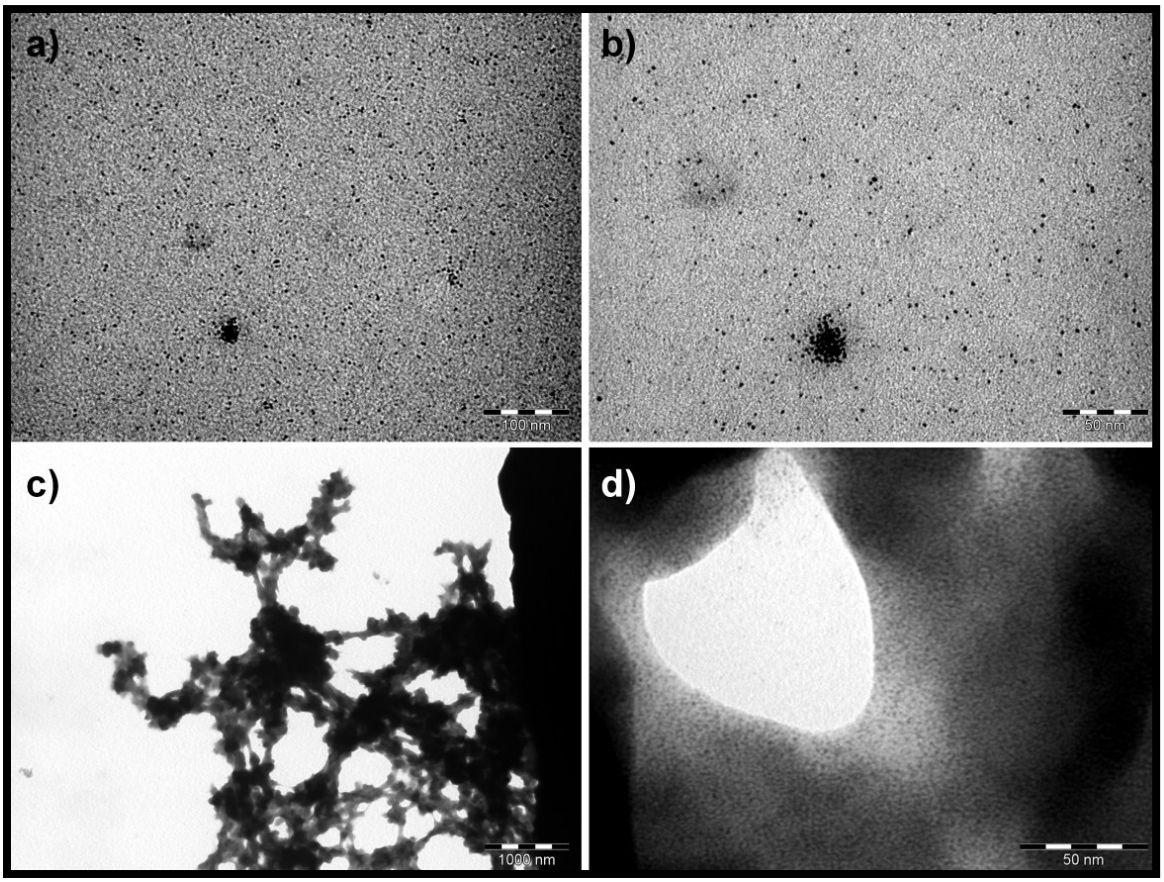

Fig. S9 TEM Images of oxidized a-b) alloy type RuRe/PVP NPs and c-d) core-shell type RuRe/PVP NPs.

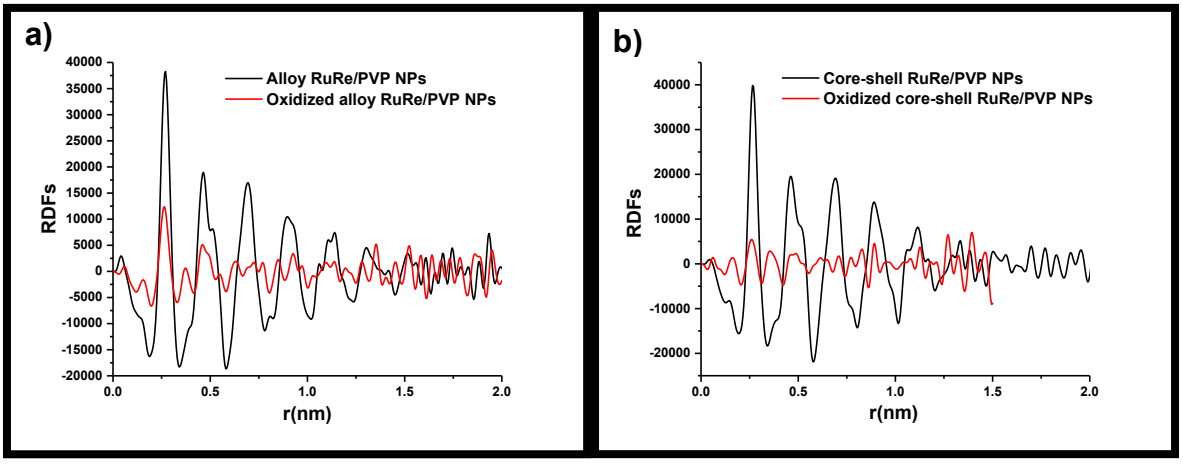

Fig. S10 RDFs of a) alloy and b) core-shell type RuRe/PVP NPs before and after oxidation.